Reviews on Advanced Materials and Technologies, 2024, vol. 6, no. 4, pp. 194–213
DOI: 10.17586/2687-0568-2024-6-4-194-213

# Synthesis of Si/G Composite Anodes for Lithium-Ion Batteries: A Review

**A. Azaizia**[*], **M.V. Dorogov**

Institute of Advanced Data Transfer Systems, ITMO University, Kronverkskiy pr., 49, lit. A, St. Petersburg, 197101, Russia

**Article history**

Received December 03, 2024
Accepted December 26, 2024
Available online December 30, 2024

**Abstract**

By overcoming significant performance constraints, recent developments in silicon/graphene (Si/G) composite anodes have shown promise for revolutionizing lithium-ion batteries. Although silicon has a remarkable theoretical capacity, structural instability results from its large volume growth during cycling. Though it lacks the potential for high-energy applications, graphene, which is well-known for its exceptional mechanical flexibility and electrical conductivity, enhances the qualities of silicon. By combining these materials, Si/G composites have demonstrated impressive gains in rate performance, structural stability, and capacity retention, providing a promising avenue for next-generation energy storage technologies. High-performance Si/G composites have been made easier to create by advancements in scalable synthesis processes like sol-gel processing, chemical vapor deposition, sophisticated self-assembly techniques and Hummer's method. With an emphasis on cutting-edge silicon-based anodes, carbon composites, and workable techniques for acquiring and altering silicon anodes, this review seeks to examine the most recent developments and unsolved issues in the advancement of lithium-ion batteries. In order to address the needs of contemporary high-capacity applications and expedite the integration of Si/G composites into next-generation energy storage systems, these insights are crucial.

*Keywords:* Lithium-ion batteries; Silicon-based anodes; High-capacity energy storage; Cycling stability

## 1. INTRODUCTION

The development of lithium-ion batteries (LIBs) in recent years has transformed energy storage technology, having an impact on many industries including portable electronic gadgets, electric vehicles, and large-scale storage systems. Because of their large capacity, lengthy lifespans, and environmental friendliness, LIBs have been widely adopted. However, there is an urgent need to create next-generation LIBs with even better energy and power densities due to the fast-rising demands on the energy market [1]. The lithium-ion transport between the anode and the cathode forms the basis of a LIB as the power supply, and the $Li^+$ insertion ability of the anode is the main factor that determines its performance [2]. This is why scientists have many resorted to the invention of many advanced materials to enhance the proprieties of these batteries [1].

Before battery fabrication, it is essential to analyze characteristic parameters like reducing power, conductivity, chemical/mechanical/thermal stability, structural defects, and morphology of anodes. This analysis helps comprehend how these parameters influence the operational dynamics of cells. The optimization of these parameters is crucial for enhancing electrode performance and, concurrently, for refining the overall cell efficiency [3]. The advantages and disadvantages of important anode materials are summarized in Table 1 [4].

Over decades of ongoing research, a diverse range of anode materials has been identified and refined. Currently, LIB anode materials can be classified into three categories based on their different reaction mechanisms: intercalation materials (such as graphite and lithium titanate), conversion materials (including transition metal oxides and sulfides), and alloying materials (like silicon, tin, germanium, and antimony) [2,5]. Summary of investigated

---

[*] Corresponding author: A. Azaizia, e-mail: amaniazaizia.1997@mail.ru

**Table 1.** Advantages and disadvantages of various anodes materials. Reprinted under a Creative Commons Attribution License (CC BY) from Ref. [4], © 2022 Royal Society of Chemistry.

| Anode materials | Advantages | Disadvantages |
|---|---|---|
| Carbon | High electronic conductivity<br>Nice hierarchical structure<br>Abundant and low-cost resources | Low specific capacity<br>Low-rate capacity<br>Safety issues |
| Alloys | High specific capacity (400–2300 $mAh{\cdot}g^{-1}$)<br>Good security | Low electronic conductivity<br>Large volume charge (100%) |
| Transition metal oxides | High specific capacity (600–1000 $mAh{\cdot}g^{-1}$)<br>Nice stability | Low coulombic efficiency<br>Large potential hysteresis |
| Silicon | High specific capacity (3579 $mAh{\cdot}g^{-1}$)<br>Rich, low cost, clean resources | Large volume change (300%) |

anode materials are shown as categories and sections in Fig. 1 [3].

A. Eftekhari et al. [6] recently classified anode materials into four categories based on their operational voltage ranges. The first category consists of low-voltage materials (including group IV and V elements), which primarily achieve their delithiation capacity below 1.0 V relative to $Li/Li^+$. The second category encompasses mid-voltage materials, such as transition metal oxides and chalcogenides, which tend to reach the majority of their delithiation capacity in the voltage range of 1.0 to 2.0 V. The third category is characterized by high-voltage materials, where most delithiation occurs at voltages exceeding 2.0 V. Finally, the fourth category includes nanostructured and mixed valence materials, which exhibit a potential window varying from 0 to 3.0 V and encompasses a broad range of materials exhibiting nanostructures and mixed valences, Fig. 2 [3,6–9].

A lot of research has focused its results on the development of anode materials for LIBs, choosing the most adequate and suitable electrode materials along with their recycling techniques. H. Kim et al. [10] particularly compared silicon-based anodes with transition metal oxides and tin-based anodes. They found that transition metal oxides, such as nickel cobalt manganese (NCM) and lithium titanium oxide (LTO), offer advantages such as cycling stability and capacity retention due to their robust structural integrity. In addition, tin-based materials, such as $SnO_2$, $SnS_2$, and $SnSe_2$, have been studied extensively as a possible replacement for current anode materials in LIBs because of their high theoretical capacity compared to graphite of 372 $mAh{\cdot}g^{-1}$, corresponding to the formation of $LiC_6$, Fig. 3 [11].

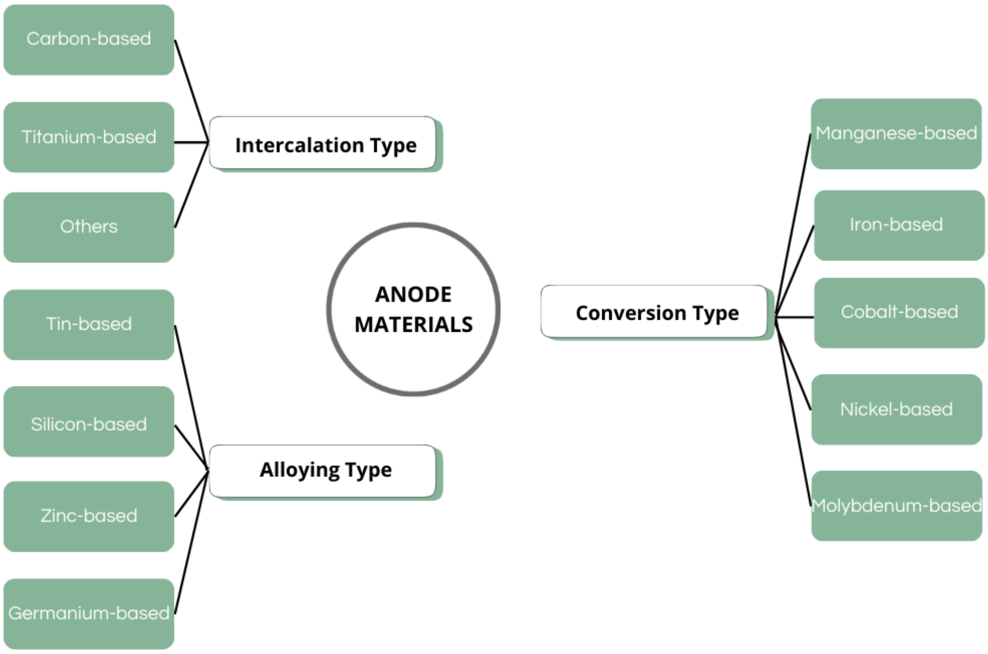

**Fig. 1.** Different types of anode materials. Adapted under a Creative Commons Attribution License (CC BY) from Ref. [3], © 2023 Elsevier.

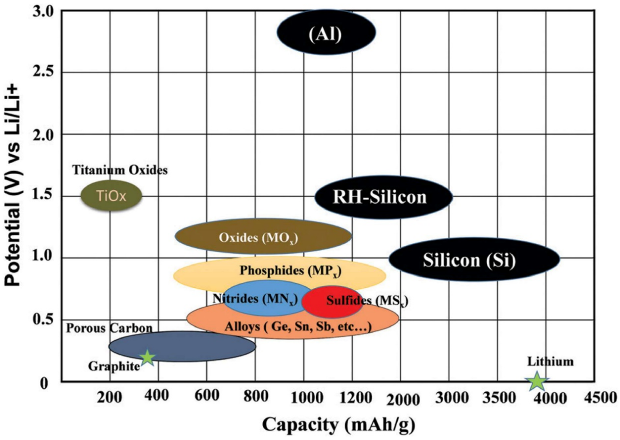

**Fig. 2.** A chart comparing different anode materials' potential and specific capacity. Reprinted under a Creative Commons Attribution License (CC BY) from Ref. [3], © 2023 Elsevier.

The major problem associated with using these materials is the excessive volume charge during the lithiation-delithiation process [11]. This problem has been successfully reduced by creating intermetallic metal composites. G. Toki et al. [11] found that silicon-based anodes, especially when combined with carbon composites, deliver a distinct advantage [12,13].

In this review, we explore the latest achievements and unresolved challenges in advancing LIBs, with a focus on innovative silicon-based anodes, carbon composites, and feasible methods for obtaining and modifying silicon anodes.

## 2. SILICONE VS GRAPHITE ANODES FOR LIBs

Silicon (Si) holds a prominent place in the periodic table as the second most abundant element on earth, making up ~28% of the planet's crust. Its abundance and exceptional physical properties have rendered it indispensable in various fields, particularly in the realm of modern electronics. While Si has undoubtedly played a transformative role in microelectronics and digital technology, the growing demand for energy storage solutions in the face of climate change and the transition to renewable energy sources has prompted a shift in focus. In recent years, researchers and engineers have been exploring alternative applications for Si beyond its traditional use in electronic devices. One such groundbreaking prospect lies in the realm of energy storage systems, particularly in LIBs [1]. In this area Si has attracted a lot of attention as anode material due to its very high theoretical specific capacity at room temperature compared to that of the commonly used carbonaceous anodes (Table 2), and due to Si atom able to form a connection with 3.75 lithium ions ($Li_{3.75}Si$) [1,14]. Additionally, Si has a higher lithiation potential compared to graphite (~0.4 V vs. ~0.2 V relative to $Li/Li^+$); this prevents lithium plating and dendrite growth, Fig. 2 [1].

Despite these advantages, several inherent issues hinder its commercialization. One major challenge is the significant volume expansion of over 300% that Si undergoes during the lithiation process, which can lead to mechanical

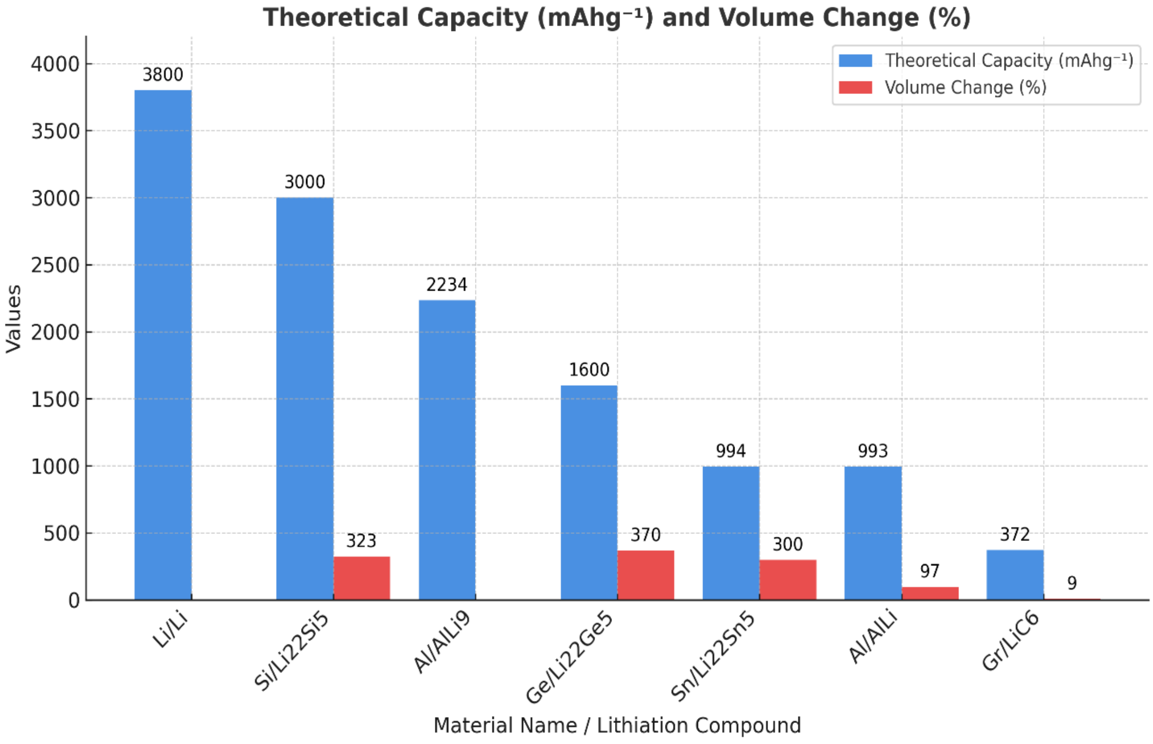

**Fig. 3.** Lithiation characteristics of different anode materials [11].

**Table 2.** A comparison of SEI formation on the silicon electrode and other common electrodes in lithium-ion batteries, highlighting their composition, formation mechanisms, impact on performance, and specific challenges [19].

| Electrode type | SEI Composition | SEI Formation mechanism | Impact on performance | Challenges with SEI |
|---|---|---|---|---|
| Si anode | $Li_2Co_3$, $Li_2O$, organic compounds, lithium alkoxides | SEI forms due to electrolyte reduction, with significant volume expansion (300%) | SEI stabilizes the surface but cracks with volume changes, leading to capacity fading | Continuous SEI breaking and reforming due to large volume changes causes excessive lithium consumption |
| Gr anode | $Li_2Co_3$, LiFe, organic carbonates | Form at low potentials (08–01 V) due to electrolyte reduction | Provide stability by passivating the surface, minimizing further decompositions | SEI thickens over cycle, reducing conductivity and causing gradual capacity fade |
| LiMe anode | $Li_2O$, $Li_2Co_3$, LiFe, Organic compounds | Forms instantly upon contact with electrolyte | SEI critical for limiting dendrite, growth improving safety | SEI instability leads to dendrite formation, causing safety hazard (e.g, short circuits) |

stress and the subsequent pulverization of the silicon powder. This expansion also results in the detachment of the conductive matrix from the active Si surface, negatively impacting its electrochemical performance. During initial lithiation, a solid-electrolyte interphase (SEI) forms on the Si electrode due to the decomposition of the electrolyte. While this SEI layer facilitates lithium-ion conduction, it limits electron flow, thereby reducing electrolyte consumption and improving the cycling performance of LIBs. However, the expansive nature of Si results in an unstable SEI that is susceptible to cracking and reformation on the Si surface. Consequently, this unstable SEI leads to continuous lithium consumption, ultimately depleting the electrolyte and lowering the initial Coulombic efficiency (ICE), Table 2 [15].

Furthermore, due to its stable crystalline structure, silicon, which has limited conductivity of approximately $10^{-3}$ S/cm at 25 °C, faces significant challenges related to electron conductivity, particularly under various unstable configurations [16–18].

To resolve these problems, researchers have explored many solutions, such as Si at the nanoscale, utilizing forms such as nanoparticles (NPs), nanowires, and nanotubes to address volume expansion that occurs during lithiation [20,21]. They have also developed Si electrode composites, including Si/graphene (Si/G) [22], transition-metal oxide composites [23,24], and Si alloy composites [25,26], to further mitigate the challenges associated with volume expansion. Table 3 summarizes the electrical conductivity values of various anode materials used in LIBs, including Si, carbon (C), Si/C composites, titanium (Ti), Si NPs, nanowires, nanotubes, Si/G composites, transition-metal oxide composites, and Si alloy composites.

Additionally, enhancements in the quality of the solid-electrolyte interphase, along with the optimization of chemical additives and the upgrading of electrolytes and adhesives, have been recognized as crucial factors for improving performance [1].

In Ref. [1] graphene has been incorporated into anode materials to serve as an ideal conductive matrix; in this case scientists, combined 2D graphene with Si. The Si/G composites emerge as promising solutions to overcome the limitations of Si as a standalone anode material. Integrating Si into graphene allows these composites to capitalize on the synergetic advantages offered by both materials. Graphene, with its thickness of ~3 nm (twice the carbon-carbon bond length), facilitates efficient electron transport throughout the electrode and accommodates the volume expansion of Si during lithiation. This feature mitigates the detrimental effects of Si’s volume changes, ultimately enhancing the cycling stability and rate capability of Si/G composites, making them highly desirable for high-performance LIBs.

Another critical factor is the performance at various temperatures and cycling conditions. Research indicates that Si/G composites can remain stable over multiple cycles, in contrast to some alternatives that may exhibit significant degradation or diminished capacity retention under similar conditions [36,37].

J. Reslan et al. [1] found that the formation of a SEI layer on Si electrodes is another challenge. While the SEI allows for lithium-ion conduction, it can inhibit electron transport due to the limited conductivity of the layer. Additionally, as Si expands, the SEI can crack and become unstable, leading to continuous electrolyte consumption and diminishing effectiveness over successive charge-discharge cycles [1]. In order to understand the electrical conductivity J. Saddique et al. [38] made a mini review about the opportunities and challenges of nano-Si/C composites in LIB, where they found that an important advancement in Si-based materials is the development of porous nano-Si architecture, which exhibits excellent structural characteristics, reduces the

**Table 3.** A comparative overview of the electrical conductivities of various anode materials utilized in lithium-ion batteries, showcasing the diversity and potential of each type for optimizing battery performance.

| Anode Material | Electrical Conductivity (S/m) | Notes | Ref. |
|---|---|---|---|
| Graphite | $10^3$ to $10^5$ | Excellent conductivity; widely used in commercial applications | [27] |
| Graphene | $10^5$ to $10^6$ | Excellent conductivity; widely used in commercial applications | [27] |
| Carbon Nanotubes | $10^4$ to $10^6$ | Very high conductivity, often used as additives to improve conductivity | [27] |
| Silicon | $10^3$ to $2 \cdot 10^{-2}$ | Conductivity varies by form (micron/nano) and presence of conductive additives | [28] |
| Titanium | $10^5$ | High conductivity; primarily used in composite structures for performance enhancement | [29] |
| Silicon Nanoparticles | $10^{-3}$ to $2 \cdot 10^{-2}$ | The presence of conductive additives enhances conductivity | [30] |
| Silicon/Carbon | $10^{-2}$ to 1 | Provides enhanced conductivity and stability through carbon matrix | [28] |
| Silicon nanowires | $10^{-3}$ to $10^{-2}$ | Conductivity can vary based on structure and additives used | [31] |
| Silicon nanotubes | Similar to silicon; generally low conductivity | Typically integrated with other materials for synergetic effects | [32] |
| Silicon/Graphene | $10^{-2}$ to 1 | Enhanced conductivity due to graphene's presence, aiding electron transport | [33] |
| Transition metal oxide composites | $10^{-2}$ to $10^{-1}$ | Conductivity can vary significantly based on specific materials and phases | [34] |
| Silicon alloy composites | $10^{-2}$ to 1 | Generally better than pure silicon alone, often enhanced with carbon materials | [35] |

volume expansion, provides sufficient channels for ion transportation, and improves the cycling stability and rate capability. Due to irreversible chemical reactions (or parasitic reactions) during the first cycles, a large initial capacity loss usually occurs, which causes the excessive consumption of Li ions in electrolyte. The effective way to overcome this issue is to use prelithiation approaches.

Recently, M. Khan et al. [39] provided a thorough review of various prelithiation techniques for Si-based anodes, evaluating them based on factors like operational simplicity, cost, stability, safety, and compatibility with current manufacturing processes. Alongside advancements in nanoporous architectures and prelithiation strategies to enhance electrochemical performance, significant progress has been made in developing new binders and electrolyte additives over the past decade. These innovations have notably improved the structural integrity and cycling performance of silicon-based anodes, as well as increased ICE and stabilized the SEI.

Scientists have explored various synthesis methods to form Si/G composite anodes, nanosheets (graphene synthesis routine) and variables in assembly methods (direct mixing, chemical bonding, and physical attraction). Due to the large variation in synthesis conditions and lack of complete information, comparative study to identify desirable properties of graphene for Si/G composite anodes based solely on literature study is not feasible. It is critical to isolate certain properties as was done in some preliminary work by J. Liang et al. [40].

In Ref. [39] Si NP size and surface treatment were maintained constant while the graphene properties were varied by different graphene oxide reduction conditions. So, when Si is used as the anode, carbon coating is needed. Si/G nanocomposites are considered one of the most promising anode materials for next generation high energy density LIBs. Many studies have explored various synthesis methods to form Si/G composite anodes. To make Si/G composites viable for commercial applications, synthesis methods must be scalable, reproducible, and cost-effective [39].

However, current fabrication techniques often result in inconsistencies in material properties, which negatively impact electrochemical performance. Therefore, developing innovative synthesis approaches that enhance the uniformity and quality of Si/G composites is crucial for practical use.

Y. Cen et al. [41] explored various fabrication methods for producing Si/G nanocomposites with promising electrochemical properties. However, several challenges remain: (1) the high cost of synthesizing nano-sized Si and graphene nanosheets, (2) low electrode loading weight, and (3) unsatisfactory cycling performance due to volume expansion. Additionally, the quality of the carbon materials used in Si/C composites significantly influences the electrochemical performance of the resulting anode and requires further investigation [41].

Despite extensive research and significant advancements in this field, several challenges remain unresolved. F. Wang et al. [19] investigated the issues of volume expansion and material pulverization in Si-based anodes. They found that during lithium insertion and extraction, Si undergoes substantial volume expansion—ranging from 300% to 420%—which leads to severe pulverization and loss of electrical contact. This causes capacity degradation and shortens the cycle life of the anode. While nanostructured Si is designed to mitigate these issues, accommodating such drastic volume changes remains a significant challenge. Moreover, forming a stable SEI is crucial for maintaining the efficiency and longevity of Si anodes. However, the continuous volume fluctuations during cycling cause cracking and instability in the SEI, leading to low Coulombic efficiency and hindering ionic transport. This, in turn, negatively affects the overall electrochemical performance of LIBs. Additionally, their study highlighted that the use of nanosized Si and Si/G composites often results in low tap density, which limits mass loading and reduces areal capacity. The excessive interparticle space in these nanomaterials leads to poor electrode packing, further compromising performance [19].

Even with the incorporation of graphene, Si's intrinsic electrical conductivity is limited, which can hinder efficient charge transfer within the anode. While graphene enhances conductivity, optimizing the Si/G interface for maximum electron transport remains an area requiring further exploration [11].

### 2.1. Pristine silicone anodes

Si particles with diameters below 150 nm have been shown to maintain structural integrity during repeated lithiation/delithiation cycles, as the reduced stress on these particles helps prevent rapid capacity decay and enhances long-term cycling performance. In particular, Si nanowires with an average diameter of 89 nm achieved a high discharge capacity of 3193 $mAh \cdot g^{-1}$ at a C/20 rate, accompanied by an initial Coulombic efficiency of 73%. Importantly, the lithium storage capacity of these Si nanowires remains stable with nearly no degradation after 10 cycles, attributed to their intact structure following repeated charge and discharge processes [21,42].

Silicon nanoparticles (SiNPs) can be effectively produced through ball milling of Si powders, which is garnering significant interest due to its cost-effectiveness compared to more expensive synthesis methods like chemical vapor deposition (CVD) using silane ($SiH_4$) precursors, with costs of approximately 2 euros per kg for ball milling versus 100 euros per kg for CVD. However, from an industrial perspective, the use of NPs presents several challenges, including issues related to volatility, inhalation hazards, and explosion risks. Despite these challenges, efforts are being made to harness the advantages of nanomaterials [1,43].

In Ref. [44] it is highlighted for the first time that extended ball milling of pure Si is a powerful and low-cost approach for producing micro-sized, nanostructured Si particles that exhibit better electrochemical performance than expensive nanosized Si powders. The researchers used commercial micrometric Si (99.9%, 1–5 microns) as the starting material, where the Si powder was combined with three stainless-steel balls. All the details are explained in their review [44].

The electrodes made from ball-milled Si particles mixed with binders demonstrated an irreversible capacitance of 1170 $mAh \cdot g^{-1}$ after more than 600 cycles, with a Coulombic efficiency exceeding 99% [1]. This impressive electrochemical performance is attributed to the presence of nanocrystalline domains within the submicron particles and the high concentration of grain boundaries, which accelerate $Li^+$ diffusion in the Si anode. Finally, the authors credit the success of the microsized Si materials to three strategies: (i) using nanocrystalline (ball-milled) Si powder for smoother phase transitions during cycling; (ii) using a carboxymethyl cellulose (CMC) binder prepared in acid, which strengthens the covalent bonding between the binder and Si particles; and (iii) incorporating fluoroethylene carbonate + vinylidene carbonate (FEC + VC) additives in the electrolyte to reduce electrolyte decomposition at the Si surface. These combined strategies likely explain why earlier ball-milled Si materials without such enhancements were less successful [1,44].

A promising strategy to address the volumetric expansion issues associated with SiNPs is the incorporation of Si-C composite materials in various structural forms, including core-shell, hollow-shell, and yolk-shell configurations [1,45].

As an illustration of these composite anodes, in Ref. [46] single-crystal *n*-type and *p*-type silicon nanowires (SiNWs) have been prepared and characterized by electrical transport measurements. Laser catalytic growth was used to introduce controllably either boron or phosphorus dopants during the vapor phase growth of SiNWs. SiNWs were synthesized using the laser-assisted catalytic growth method, their studies show it is possible to incorporate high dopant concentrations in the SiNWs and to approach the metallic regime. Temperature dependent measurements made on heavily doped SiNWs show no evidence for single electron charging at temperatures down to 4.2 K, and thus suggest that the SiNWs possess a high degree of structural and doping uniformity. In the other studies, porous Si-C composite particles present a viable solution to address the limitations associated with non-porous Si-C materials. The presence of preexisting pores facilitates the necessary volume for Si expansion while enabling rapid transport of lithium ions, which is essential for efficient battery performance. Furthermore, the carbon component in these composites enhances the formation of the solid/electrolyte interface, contributes to structural integrity, and ensures high electrical conductivity. When engineered effectively, porous Si-C composite particles can maintain their size and shape during cycling, which is crucial for industrial applications, particularly since commercial battery cells have very limited space for anode expansion [47].

However, the low-cost synthesis of such composites is not a trivial task. In this context, A. Magasinski et al. [45] used the bottom-up assembly to develop Si-C porous composite powders with high capacity, stable performance and particle size comparable to that of milled graphite (15–30 μm). They developed a CVD synthesis process to create SiNPs on the surface of carbon black NPs, which form short branched chains during high-temperature pre-annealing. The resulting 0.5–1 μm multibranched nanocomposite, subsequently self-assembles into large porous spherical granules during the atmospheric pressure CVD deposition of carbon.

The size of the deposited Si nanoparticles is determined by the duration of the Si CVD deposition process, as well as the pressure and temperature settings within the deposition system. Additionally, the dimensions of the branches in the nanocarbon and the size of the deposited SiNPs influence the pore size of the synthesized composite. Consequently, the carbon CVD process parameters and the initial size of the branched carbon particles play a crucial role in controlling the particle size, pore size, and composition of the composite [48]. Anodes made out of these porous Si-C composite exhibit exceptional electrochemical performances such as a specific capacity of 1950 $\mathrm{mAh \cdot g^{-1}}$ at C/20 (six times higher than that of conventional graphitic anodes) and a volumetric capacity of 1270 $\mathrm{mAh \cdot cm^{-3}}$ at C/20 (620 $\mathrm{mAh \cdot cm^{-3}}$ for graphitic anodes) [1,48].

There are numerous Si anode synthesis methods for LIBs that have not been addressed in this review. In Table 4, a comparison of various Si anodes is presented, detailing information on fabrication methods, particle sizes, and their electrochemical performance. Each type of anode possesses distinct advantages, which have been previously explained to highlight the reasons for researchers' focus on these materials and their published findings. Upon analyzing the table, it is evident that Si NWs synthesized using specific methods demonstrate excellent electrochemical performance, exhibiting consistent capacity across numerous cycles. In contrast, other materials such as SiNPs or thin films show performance variations that largely depend on their fabrication methods. Notably, most other anode materials tend to experience a capacity loss of approximately 50% after prolonged cycling [1].

Similar results are observed on another type of anode materials. The anode materials made of copper oxide nanowires that we studied earlier also show results higher than those made of copper oxide NPs [24,49]. Calculations show that such one-dimensional materials can more easily withstand high mechanical stresses and deformations that arise during the process of lithiation and delithiation [50,51].

## 2.2. Graphene anodes

Graphene has been clearly identified as one of the candidates to compete with the dominating graphitic material for manufacturing anode electrodes [1]. Graphene is a two-dimensional material comprised of a single or a few atomic layers of $sp^2$-bonded hexagonal carbon. It showcases exceptional physical properties, including a high transparency of 98.4% and superior electrical and thermal conductivity measured at 85000 S/m, and 5000 $\mathrm{W\ m^{-1}\ K^{-1}}$, respectively [10]. Additionally, graphene features a remarkable specific surface area of 2630 $\mathrm{m^2\ g^{-1}}$ and an optical absorption of only 2.3% [10,52]. Additionally, its exceptional diffusion coefficient surpasses that of graphite, enabling faster and more efficient transport of lithium ions within the battery structure. When incorporated into anode materials, graphene serves as an outstanding conductive network, facilitating rapid electron transport throughout the electrode, thus enhancing the overall performance of the battery [1]. Moreover, the diverse forms in which lithium can be incorporated into graphene, including both sides and within the material's defects, offer opportunities for further exploration and optimization of LIB designs, emphasizing the versatility and potential of graphene in advancing the next generation of energy storage technologies [1]. The diverse forms in which lithium can be incorporated into graphene—both on its surfaces and within the material's defects—provide significant opportunities for further exploration and optimization of LIB designs. This versatility underscores the potential of graphene to advance the next generation of energy storage technologies. The ability to exploit various incorporation methods enhances the efficiency and overall performance of LIBs, making graphene a promising material in this field [52,53].

**Table 4.** Si-based lithium-ion battery anodes. Reprinted under a Creative Commons Attribution License (CC BY) from Ref. [1], © 2024 Wiley-VCH GmbH.

| Anode materials | Method used | Particle size (nm) | Initial discharge (mA·g$^{-1}$) current density (A·g$^{-1}$) | Capacity/ Cycles/ Current density (mAh·g$^{-1}$) (A·g$^{-1}$) | ICE (%) |
|---|---|---|---|---|---|
| Si thin films | Electrodepositing | 50–100 | 2550/036 | 2800/80/3.6 | 53 |
| Si thin films | Magnetron sputtering | 100–300 | 3134 at 0.025 C | 1317/500 at 0.5 C | 87 |
| SiNPs | Chemical synthesis | < 70 | 1157/0.05 | 452/50/0.05 | 76.3 |
| SiNPs | Ball milling | 50 | 3075/0.05 | 804/400/1 | 84.5 |
| SiNPs | Ball milling | 10 | 3250/0.48 | 1600/600/0.48 | 81 |
| SiNPs | Ball milling | 150–200 | 2196/0.1 | 1480/100/0.1 | 67.3 |
| SiNPs | CVD | 10–30 | 1950/0.0975 | 1500/100/1.95 | 86 |
| SiNPs/$SiO_2$ | Ball milling | 50–70 | 805.57/0.2 | 704.79/500/0.2 | 88 |
| SiNWs | CVD | 3–10 | 3720 at C | 2670/50 at 1.3C | 65 |
| SiNWs | Vapor liquid solid | < 100 | 2836 at 0.1C | 2600 after 20 cycles | 93.7 |
| SiNWs | CVD | 10–50 | 1300/0.85 | 1060/100/0.85 | 86.2 |
| SiNWs | Boron doped | 100 | 3038/0.4 | 2000//250/2 | 89 |
| SiNWs | CVD-spray coating operation | 30 | 3750/0.00025 | 2950/200/0.00025 | 78 |
| SiNWs | ECR-CVD / MCEE | 10–50 | 2911/0.25 mA·cm$^{-2}$ | 2445/25/0.25 mA·cm$^{-2}$ | 95 |
| SiNWs | Magnesiothermic reduction | < 23 | 1586/0.2 | 1038/170/0.2 | 48.3 |
| SiNWs | DC-arc discharge | 20 | 2553/0.1 | 441.7/10/0.1 | 49 |
| SiNWs | Liquid oxidation and exfoliation | < 10 | 1375/0.1 | 596/1800/1 | 61.6 |
| Si nanotubes | Electrospinning/CVD | 10 | 650 at 12 C | 570/6000 at 12C | 76 |
| Si hollow spheres | CVD | 100–400 | 2725 at .01 C | 1420/700 at 0.5C | 77 |
| Mesoporous Si | Magnesiothermic reduction | 20–120 | 4819/0.05 | 1004/50/0.05 | 64.2 |
| Porous Si membrane | HCl-leaching and water-rinsing | 25 | 3420/0.1 | 1220.2/100/1 | 71.8 |
| Porous Si | MCEE of Si powders | 10–50 | 2530 at 0.1C | 200/50 at 0.2C | 69.3 |
| Porous Si | Reduction of mesporous $SiO_2$ | 150 | 2416/0.1 | 1600/100/0.1 | 73.7 |
| Porous Si | Magnesiothermic reduction of rice husk | > 200 | 2790/0.084 | 1500/300/2.1 | 70 |
| Porous Si | Magnesiothermic reduction of diatomite | 100 | 1826/0.05 | 240/30/0.5 | 68.5 |

In Ref. [53] they present a facile and effective method, combining mechanical agitation, ultrasonic dispersion, and dispersant surface modification, to produce high mass concentration (1%) graphene conductive slurries as conductive agent for LIBs. The dispersant CMC significantly enhances the dispersion and stability of graphene in aqueous solutions. When used as a conductive agent in LIBs, the graphene slurry (G-CMC) demonstrates impressive battery performance, achieving a first charge and discharge capacity of 1273.8 mAh·g$^{-1}$ and 1723.7 mAh·g$^{-1}$, respectively, with a Coulomb efficiency of 73.9% at a current rate of 100 mA·g$^{-1}$. Additionally, the anode exhibits a capacity retention rate of 84% (1070.2 mAh·g$^{-1}$) after 100 cycles at a current of 200 mA·g$^{-1}$. This strategy, which combines physical dispersion with dispersant modification to formulate graphene slurry, shows significant potential for application as a conductive agent in LIBs [53].

Methods for producing high-quality graphene have been thoroughly investigated to fulfill the demands of anode applications in LIBs [1]. Several techniques have been developed for the large-scale synthesis of graphene, ensuring its readiness for commercial applications. Notable methods include liquid-phase exfoliation, which efficiently separates graphene from graphite; chemical reduction of graphene oxide, which transforms oxidized graphene into high-quality graphene sheets; and CVD. Each of these techniques offers distinct advantages and is tailored to meet specific production needs, thereby enhancing the accessibility of graphene for various applications [54].

CVD is a prominent method for producing high-quality graphene sheets. In this process, hydrocarbons are thermally decomposed on a metallic substrate, resulting in the formation of graphene layers with controlled thickness and large surface areas [55]. CVD enables scalable and continuous production, which makes it an ideal choice for industrial applications. This technique not only ensures the uniformity and quality of the graphene produced but also supports the growing demand for graphene in various technological fields [56].

K. Rana et al. [57] successfully produced freestanding and flexible graphene films, ~5–8 μm thick, through the CVD method for use as a battery anode. Notably, these graphene anodes, unlike typical ones, did not require current collectors or additives. They demonstrated a specific capacity of 350 mAh·g$^{-1}$, closely aligning with the theoretical value of graphite, and exhibited stable cycling performance for 50 cycles, even at a high C-rate (over 2 C). When applied in flexible LIBs under a bending radius of 10 mm, the anodes maintained stable initial capacity for over 40 cycles. This unique freestanding graphene, with a thickness of 5–8 μm, showcased excellent flexibility, attributed to its thinness and the absence of a need for a metal current collector, which, while also thin, cannot store lithium ions [1,57].

## 2.3. Silicone/graphene anodes

In LIBs, graphite is the most common anode material, in which lithium ions intercalate and deintercalate between the graphite layers during the charge/discharge process; however, graphite's theoretical capacity is only approximately 372 mAh·g$^{-1}$, while Si has a much higher capacity at up to 4198 mAh·g$^{-1}$. The corresponding chemical processes taking place in graphite are given by the following equations:

$$6C + Li^+ + e^- \rightleftarrows C_6Li, \quad (1)$$

$$Si + 4.4Li^+ + 4.4e^- \rightleftarrows Li_{4.4}Si. \quad (2)$$

When Si transforms into $Li_{4.4}Si$, its volume increases by about 3.8 times. Such huge expansion and repetitive stress due to expansion and shrinkage during charge and discharge cycles result in the collapse and pulverization of Si, detaching it from the electrode. To circumvent these issues, several sophisticated synthesis methodologies have been developed for Si/G composites [58].

P.B. Zhang et al. [59] successfully fabricated SiNPs/G composites using the CVD technique. SiNPs, approximately 30 nm in diameter, were employed as the active material, while copper foil (99.8% purity) served as the catalytic substrate. Graphene was utilized as the carbon matrix. The copper foil, coated with SiNPs, was then placed in the heating zone of a single-zone tube furnace, heated to 1000 °C (Fig. 4a). Lithium iron phosphate

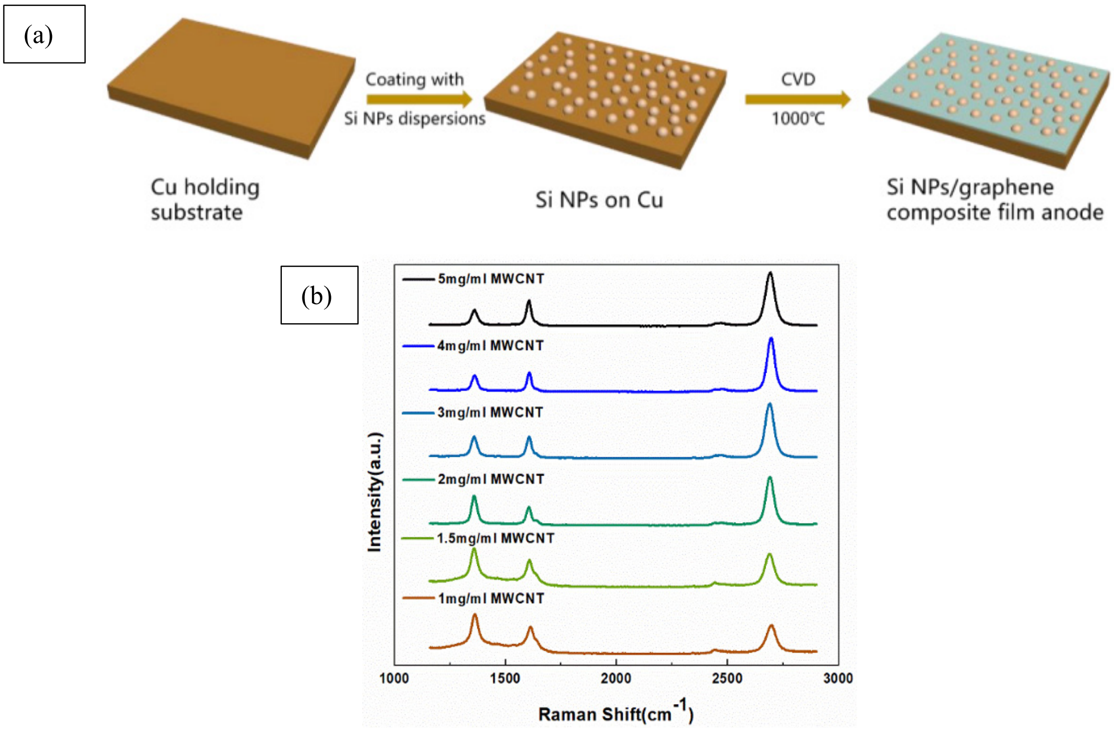

**Fig. 4.** (a) Schematic representation of CVD technique to fabricate SiNPs/G composite anodes, (b) Raman spectra of SiNPs/G composite films with different concentrations of MWCNTs. Reprinted under a Creative Commons Attribution License (CC BY) from Ref. [59], © 2019 IOP Publishing.

($LiFePO_4$) was used as the cathode material, and the electrolyte comprised a mixture of ethylene carbonate (EC), dimethyl carbonate (DMC), and lithium hexafluorophosphate ($LiPF_6$). Although additional multi-walled carbon nanotubes (MWCNTs) increased the specific surface area, which resulted in a larger consumption of $Li^+$ and the production of the SEI film at the anode, the Raman spectra of SiNPs/G with different concentrations of MWCNTs indicated that the composite film was supported. The LIB's energy density suffered because of this (Fig. 4b). Lithium-ion intercalation into the SiNPs and graphene composite film electrodes is probably the cause of the recurrent spike near 0 V in each cycle that was seen by cyclic voltammetry graphs. Nevertheless, after only six cycles, the composite anode failed [1,59].

In contrast to current methods, D. Lou et al. [33] devised an approach that involved uniformly dispersing Si and graphene NPs in liquid media with the use of a suitable surfactant. This allowed them to produce Si/G composites that were inexpensive and easily scalable. In particular, Si nanopowder (50–70 nm) and graphene nanoplatelets (4–5 layers, 8 nm thick, > 97% purity) were dissolved in deionized water using sodium dodecyl benzenesulfonate (SDBS) as a surfactant. The mixture was exposed to ultrasonication for 20 minutes at 40 watts, with an ice bath employed to chill the Si NPs. The solid was filtered and cleaned to get rid of extra surfactant, then dried for 12 hours at 80 °C in a vacuum oven before being milled into a powder (Fig. 5) [33].

According to their findings, the Si/G composite electrode outperformed pure Si electrodes in terms of electrochemical performance and cycling stability. The Si/G cell showed superior capacity retention across cycles, with 97% retention after 25 cycles and 89% retention after 50 cycles, despite the Si-based cell's initial larger capacity. The graphene structure, which permits the volume expansion of SiNPs, is responsible for this improved stability. Nevertheless, capacity loss quickened after 50 cycles, and by the 100th cycle, 62% of the Si/G electrode's original capacity was still present. As a result of testing temperature fluctuations, the Coulombic efficiency stayed over 90% and occasionally surpassed 100% (Fig. 6) [33].

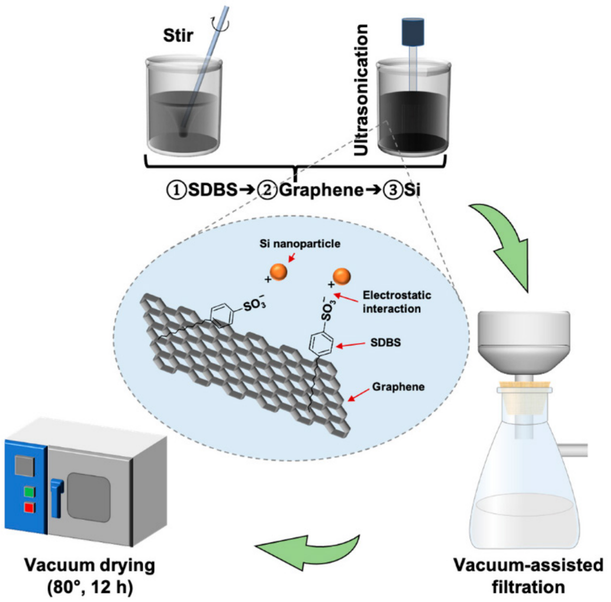

**Fig. 5.** Schematic diagram of the preparation of Si/G nanocomposite. Reprinted under a Creative Commons Attribution License (CC BY) from Ref. [33], © 2022 MDPI.

Additionally, relative to the Si electrode, the Si/G electrode displayed lower resistance, according to electrochemical impedance spectroscopy (EIS), suggesting improved conductivity and quicker charge transfer. Better mass transfer of Li ions was further suggested by the decreased Warburg resistance. The even dispersion of Si NPs and graphene, which improves conductivity and lessens the effects of volume expansion, is responsible for the Si/G composite's overall better performance [33].

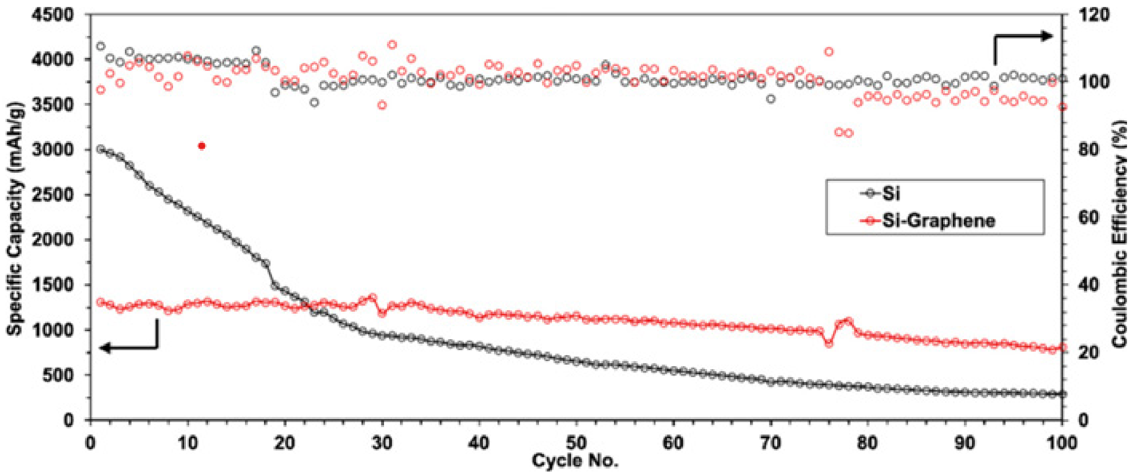

**Fig. 6.** Specific charge/discharge cycling performance of Si/G and Si anodes at a current rate of 0.1C in the first 100 cycles. Reprinted under a Creative Commons Attribution License (CC BY) from Ref. [33], © 2022 MDPI.

J.K. Lee et al. [60] created a different composite for LIB anodes in a different investigation. In order to create a silicon oxide layer, Si NPs smaller than 30 nm were first treated in the air. Graphene oxide (GO), which was created by oxidizing graphite, was then mixed with these particles. To create the Si/G nanocomposites, the mixture was reduced with 10% hydrogen in argon for one hour at 700 °C. The recently created Si/G nanocomposites showed a remarkable initial discharge capacity of about 1950 $mAh{\cdot}g^{-1}$, holding onto about 900 $mAh{\cdot}g^{-1}$ after 120 cycles at the 1000 $mA{\cdot}g^{-1}$ current rate [60].

Numerous investigations used a high graphene ratio (> 20 wt.%) and concentrated on the Si/G anode synthesis process. Y.-S. Ye et al. [61] looked into the impact of a higher graphene weight ratio in a Si/G nanocomposite. Weight ratios of 3:1, 2:1, 1:1, and 1:2 for Si/G were investigated. The Si/G ratio of 3:1 showed the finest balance between cycling performance and starting capacity. Additionally, Chabot et al. looked at the loading ratio between graphene and Si NPs. Si/G nanocomposites in the following ratios were investigated: 1:3, 1:2, 1:1, and 1:0.5. The maximum initial capacity was around 2600 $mAh{\cdot}g^{-1}$ for Si/G with a ratio of 1:0.5. Nevertheless, after 100 cycles, Si/G with a 1:1 ratio showed the maximum retention capacity of about 1000 $mAh{\cdot}g^{-1}$ [41,61].

A promising method seems to be the creation of a Si/G nanocomposite anode through a self-assembly process using GO and Si NPs. It is worth noting that three main techniques for creating graphene oxide are widely used: Brodie's, Staudenmaier's, and Hummer's methods [58].

Of these, Hummer's method is well known for yielding high-grade GO with a significant number of functional groups that contain oxygen, including hydroxyl, carboxyl, and epoxide groups [62]. Stronger bonding inside the composite is made possible by these functional groups, which greatly improve the interfacial contacts between GO and Si [63]. By increasing the number of active sites for storing lithium and enhancing conductivity generally, this better integration directly leads to the improved electrochemical performance of LIBs.

Additionally, L. Niu et al. conducted experiments focused on modulating the functional groups of GO to further enhance the electrochemical performance of Si/reduced graphene oxide (Si/rGO) anodes [63]. Their findings highlight the importance of functional group optimization in achieving superior LIB performance.

W.S. Hummers [64] created a method for producing GO by processing graphite with sulfuric acid, sodium nitrate, and potassium permanganate. This procedure was faster and safer than Brodie's and Staudenmaier's previous approaches. As a result, it has long been considered as a reference approach among researchers. For example, X. Li et al. [22] created a yolk-shell structure using a carbon/graphene double-layer-coated Si material to reduce structural degradation and improve the low inherent electrical conductivity of Si NPs. The inner carbon covering increased the surface electronic conductivity of the Si NPs, while the graphene served as flexible and conductive bridges, improving intergranular conductivity, addressing Si volume expansion, and preserving the electrode's structural integrity [22]. In short, the surface oxide layer was first removed from nano-sized Si particles by pretreating them to create the Si/C/G composites. The components were mixed in an agate mortar and heated to 90 °C for 12 hours to create carbon-coated silicon (Si/C) particles. The mixture was calcined in a nitrogen environment to create the finished composite. A modified Hummer's method was used to create GO sheets from natural graphite flakes. The Si/G composites were then synthesized using a hydrothermal method. The same procedure used for Si/G was used to create Si core/carbon/graphene (Si/C/G) composites with the materials dispersed in ethanol and subjected to ultrasonic treatment followed by thermal processing (Fig. 7) [22].

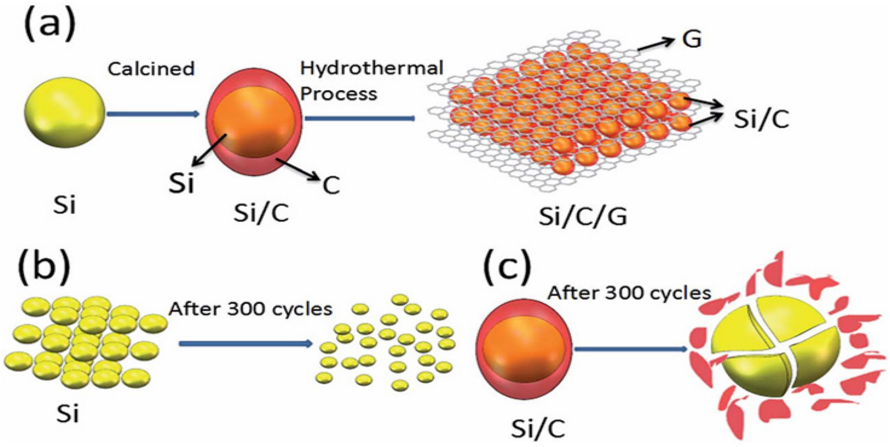

**Fig. 7.** The synthesis of the Si/C/G is shown schematically in (a), and the Si/C structure modifications after numerous cycles are shown in (b) and (c). Reprinted under a Creative Commons Attribution License (CC BY) from Ref. [22], © 2017, Royal Society of Chemistry.

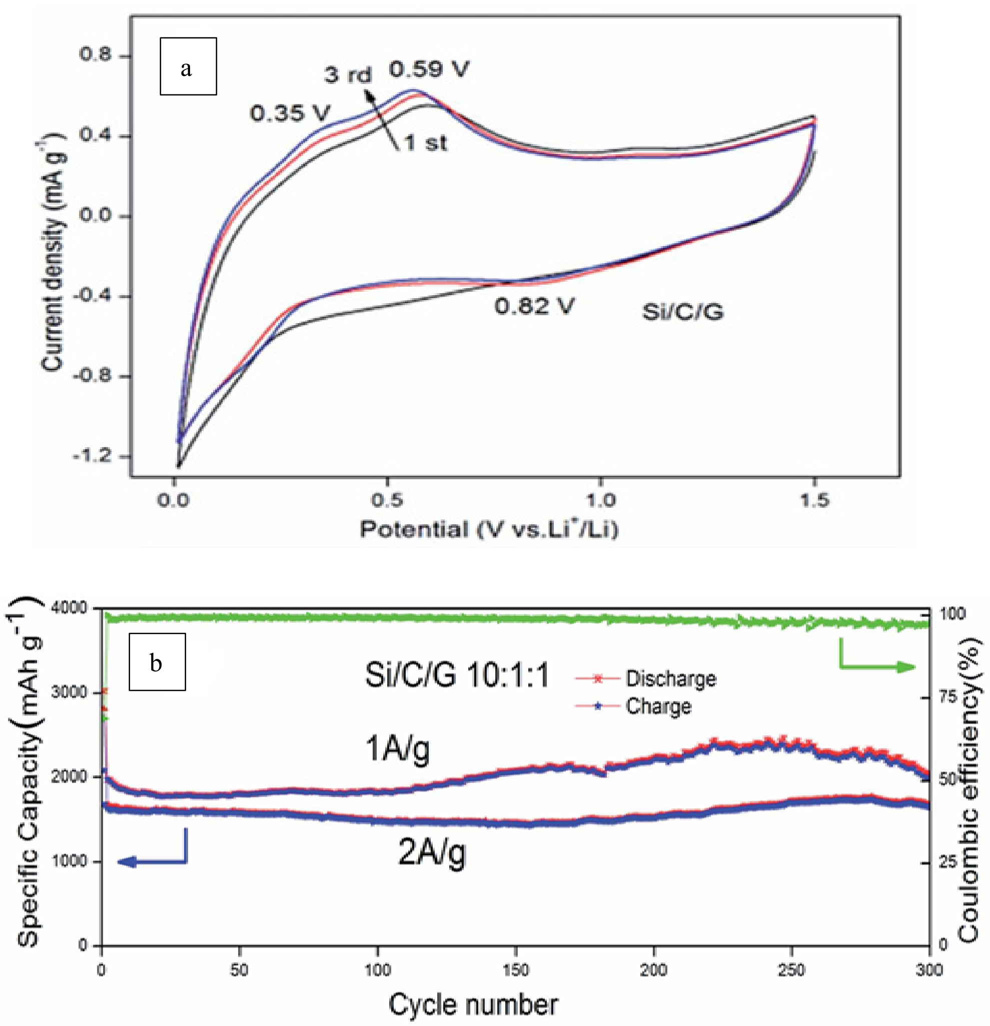

**Fig. 8.** (a) Si/C/G composite cycling performance from 0.01 to 1.5 V at a scanning rate of 0.5 mV·s$^{-1}$. (b) The Si/C/G composite electrode's discharge capacity and Coulombic efficiency at current densities of 1 and 2 A·g$^{-1}$. Reprinted under a Creative Commons Attribution License (CC BY) from Ref. [22], © 2017 Royal Society of Chemistry.

According to their results, cyclic voltammetry (CV) of the Si/C/G composite revealed distinct lithiation/delithiation peaks, as well as the creation of a stable SEI layer (Fig. 8a). EIS showed that the Si/C/G composite had the lowest charge-transfer resistance, indicating increased conductivity due to the amorphous carbon layer and graphene [22].

Regarding specific capacity and stability, the Si/C/G composite demonstrated high specific capacity and stability, with an initial discharge specific capacity of 3366 mAh·g$^{-1}$ and retaining 2469 mAh·g$^{-1}$ after 50 cycles. Long-cycle testing showed steady capacities of around 2000 mAh·g$^{-1}$ and 1600 mAh·g$^{-1}$ at discharge currents of 1 A·g$^{-1}$ and 2 A·g$^{-1}$, respectively. The Si/C/G composite outperformed previously reported Si/C composites by sustaining discharge capacities exceeding 2000 mAh·g$^{-1}$ after 300 cycles (Fig. 8b). Lastly, no notable morphological changes were found in the SEM study conducted after 700 cycles, indicating the Si/C/G composites (Fig. 9) [22].

In a similar context, Y. Du et al. [65] synthesized GO from graphite using the Hummer's method. The graphene sheets were then in-situ loaded with nanosized $SiO_2$ using tetraethyl orthosilicate (TEOS). After that, they used a magnesium thermal reduction technique to create Si/G composites. They also created Si/G samples for comparison by physically combining graphene and Si NPs [65].

X-ray diffraction and Raman spectra verified the effective conversion of $SiO_2$ into Si based on their findings. The absence of the distinctive graphene peak was probably caused by the Si NPs' great dispersion of graphene sheets. Along with graphene's D and G bands, Raman spectra showed clear Si peaks. The structural results are consistent with the electrochemical results, which showed that the Si/G composite had an ICE of 62% and an initial discharge capacity of 2808 mAh·g$^{-1}$ and a reversible capacity of 1743 mAh·g$^{-1}$ [65]. The development of the SEI and the breakdown of $SiO_2$ were identified as the causes of the irreversible capacity loss. Furthermore, even at a high current

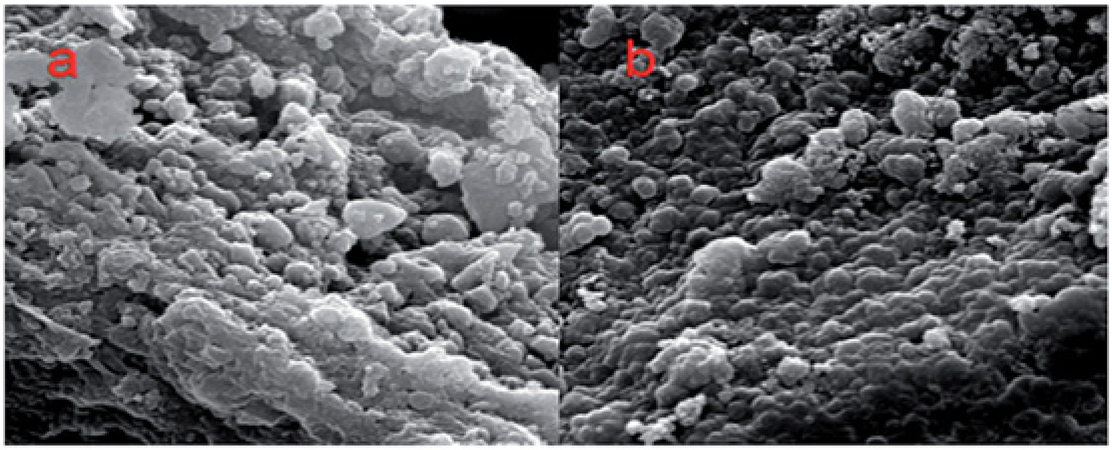

**Fig. 9.** Si/C/G electrode SEM pictures before and after 700 cycles are shown in (a) and (b). Reprinted under a Creative Commons Attribution License (CC BY) from Ref. [22], © 2017, Royal Society of Chemistry.

rate of 5 A·g$^{-1}$, the composite retained a high reversible capacity of 450 mAh·g$^{-1}$, showcasing excellent rate performance. Additionally, after 120 cycles at 100 mA·g$^{-1}$, the composite maintained 79% of its capacity, which was higher than the Si/graphene mixture's 24% and pure Si's 6% after 100 cycles [65]. An initial reversible capacity of 1750 mA·g$^{-1}$ at a current rate of 100 mA·g$^{-1}$ and exceptional cycling stability, sustaining a capacity of 1374 mA·g$^{-1}$ over 120 cycles, were among the exceptional qualities of the composite that this synthesis process produced [65].

Conversely, rGO can be added by chemical reduction with reagents like hydrazine or by thermal reduction of GO. As an alternative, CVD can be used to directly produce graphene. These techniques do have some serious drawbacks, though: Si particles are expensive, the CVD process necessitates large-scale, costly equipment that is inappropriate for mass manufacturing, and hydrazine is extremely poisonous, making it unsuitable for industrial use [53]. Building on their previously published method [58], I. Imae et al. suggested a modified way to create Si/rGO composites in this context. They reduced both GO and silica using a technique called magnesiothermic reduction, which is a thermal reduction process incorporating magnesium. TEOS was added to an aqueous dispersion of GO (5 mg·ml$^{-1}$) after GO was prepared, and the mixture was agitated for a whole day. The resultant GO/silica composite was then mixed with magnesium powder, sonicated to distribute it, and dried at 80 °C. The resulting Si/G composites were purified by using hydrochloric acid to remove magnesium-based byproducts (such as MgO and $Mg_2Si$) and hydrofluoric acid to remove any remaining silica after the dried samples were heat-treated at 800 °C under vacuum. Because it does not require alcohol solvents or the acid or base catalysts that are frequently used in TEOS sol–gel processes, this synthesis approach is notable for its ease of use and environmental friendliness [58].

Table 5 provides an overview of documented studies on Si/G nanocomposites to help understand the effect of synthesis methods on the properties and functional performance of Si/G composite anodes for LIBs [41].

A simple and promising method for creating anode materials is to coat graphene with Si NPs by synthesizing the Si/G nanocomposite anode using a self-assembly technique. The first step in the procedure is the creation of GO sheets, which are usually accomplished using Hummer's technique, which oxidizes graphite to create GO. Following their dispersion in a solution, the GO sheets engage with Si NPs through van der Waals and electrostatic forces, enabling the GO to coat the Si NPs uniformly. Reduced GO, efficiently encloses the Si particles and surrounds each NP with a conductive, protective shell.

The self-assembly method has a number of important advantages. First of all, it guarantees that Si is distributed uniformly throughout the graphene network, reducing problems brought on by Si's expansion and contraction during cycling. Rapid electron transit is another benefit of the conductive graphene layer, which improves the anode's overall electrochemical performance. This synthesis approach is feasible for large-scale manufacturing since it is straightforward, scalable, and does not require complicated equipment [66].

D. Wang et al. [67] and W. Zhang et al. [68] have shown the promise of Si/G composites by doing research that demonstrates their ability to produce enhanced cycling stability and high reversible capabilities. D. Wang et al., for example, demonstrated the endurance of Si/G composites by finding that they maintained over 85% of their capacity after 300 cycles. Furthermore, the conductive graphene layer greatly enhanced rate performance, enabling the anode to support greater current densities with no capacity loss, according to W. Zhang et al. For next-generation LIBs, this Si/G composite synthesis technique

**Table. 5.** A summary of study results on Si/G graphene nanocomposites anodes. Reprinted under a Creative Commons Attribution License (CC BY) from Ref. [41], © 2018 MDPI.

| Si source | Graphene synthesis method | Graphene weight ratio | Electrode loading density (mg/cm$^2$) | Initial reversible capacity (mAh/g) | First cycle efficiency | Best capacity retention with current rate |
|---|---|---|---|---|---|---|
| SiNPs | Graphite oxidation + thermal reduction | ~40% | 2 | ~2050 | ~96% | 300th,~56%,1000mA/g |
| SiNPs | Modified Hummers method + Chemical reduction | 73.6% | NR | ~1000 | ~41% | 100th,~70.8%,50mA/g |
| SiNPs | Hummers Method + thermal reduction | 66.7% | NR | 1040 | 63% | 30th,94%,50mA/g |
| SiNPs | Thermal expansion | ~33% | NR | 2753 | ~80% | 30th,~91%,300mA/g |
| Aerosol droplets SiNPs | Crumpled reduction | 40% | 0.2 | 1175 | ~95% | 250th,~86%,1000mA/g |
| 3-D porous Si by magnesiothermic | Hummers method + thermal reduction | ~40% | NR | 1100 | ~79% | 100th,~50%,5000mA/g |
| SiNPs on graphite foam | Hummers method + thermal reduction | 15.1% | 1.5 | 1000 | 62.5% | 100th,~37%,400mA/g |
| SiNPs on 3-D tree-like graphene nanosheets (GNS) | Microwave pasma CVD | 19% | NR | 2731 | ~56% | 160th,~67%,150mA/g |
| Polyaniline(PANI)-SiNPs | Modified Hummers method + pyrolysis mthod | 26% | 0.3 | ~1500 | ~70% | 300th,~76%,2000mA/g |
| SiNPs on electrospun carbon nanofibers (CNFs) | Chemical method + thermal reduction | 0.6% | NR | 1270 | 71.2% | 50th,~91%,100mA/g |
| SiNPs on graphene hydrogel | Modified Hummers method ascorbic acid+ thermal reduction | 29% | NR | 2250 | 53% | 150th,~50%,100mA/g |
| 3D SiNWs | CVD + plasma enhanced CVD | NR | ~0.5 | ~2600 | 97% | 100th,~29%,500mA/g |

offers a potential route to producing high-performance anodes with high energy capacity, stability, and durability [67,68].

## 3. CATHODE MATERIALS FOR SILICONE/GRAPHENE ANODES

Several cathode materials, such as nickel-manganese-cobalt oxide (NMC), lithium-rich layered oxides, high-voltage spinel lithium manganese oxide ($LiMn_2O_4$), and dilithium hydroquinone have been investigated in the development of Si/G nanocomposite anodes for LIBs to improve performance and stability [69–72]. A notable example is the use of a $LiMn_2O_4$ cathode, which has been integrated with a Si/G nanocomposite anode. This combination demonstrated stable cycling performance at practical working voltages ranging between 3.2 and 4.2 V [73].

R. Hu et al. synthesized a Si/G-based nanocomposite anode using discharge-plasma-assisted milling (P-milling) in Ref. [74]. The nanocomposite with 50 wt.% Si showed good cycleability, high capacity, and an excellent high-rate capability as a lithium storage anode. After 200 cycles at a current density of 0.4 $mA\cdot cm^{-2}$, it produced a discharge capacity of 866 $mAh\cdot g^{-1}$ and a coulombic efficiency above 99.0%. For 0.02–2 V, the capacity loss over 200 cycles was a mere 0.07% per cycle. This stability was further affirmed when the anode was paired with the $LiMn_2O_4$ cathode, underscoring its practical applicability in full-cell configurations [74].

Moreover, combining Si/G anodes with $LiMn_2O_4$ cathodes in LIBs poses a number of difficulties, especially with regard to cycle life and energy density. A major obstacle is the substantial volume shift that occurs in silicon during the lithiation and delithiation procedures. Reduced cycle life and capacity fading may occur from mechanical deterioration brought on by this volumetric expansion and contraction [74]. The performance and stability of the anode across numerous cycles are further impacted by these volume variations, which also impede the creation of a stable SEI on the silicon surface [74]. Despite its high operating voltage and environmental friendliness, $LiMn_2O_4$ on the cathode side has capacity fading because of manganese dissolving into electrolyte and structural instability during cycling [74].

In another side, compared to other known Li-insertion compounds like manganese-spinel, olivine lithium iron phosphate (LFP) based nanomaterials have shown superior power (rate) performance, thermal stability, cycle life, and are thought to be relatively environmentally benign in terms of improving cathode material performance. In particular, $LiFePO_4$ (LFPO) has capacities of up to 170 $mAh·g^{-1}$, and combining it with Si-based anodes can greatly increase the total energy density [75]. In order to improve the mechanical and electrical conductivity, M.J. Loveridge et al. [75] developed a nano-sized V-doped LFP material (as a cathode) and an enhanced Si anode in 2016 by adding functionalized graphene nanoplatelets with high electrical conductivity. In their study, a cathode was created by combining carbon-coated V-LFP, carbon black, and a polyvinylidene difluoride binder solution (PVdF), which was then coated on aluminum foil using reel-to-reel or draw-down coating processes, with changes for viscosity and drying. A graphene-containing version added a few layers of graphene for improved characteristics [75]. Furthermore, experimental investigation of Si/G composite anodes reveals excellent capacity retention even at high current densities. For example, one study found that Si/G electrodes could attain a specific capacity of around 1200 $mAh·g^{-1}$ while retaining about 80% of their initial capacity after 500 cycles at a current density of 2 $A·g^{-1}$. This performance demonstrates these materials' potential for high energy densities appropriate for advanced battery applications. The $LiFePO_4$ and Si/G combination is suited for full-cell designs. A design using a $LiPF_6$-based electrolyte augmented with fluoroethylene carbonate resulted in an energy density of 250 $Wh·kg^{-1}$ and around 85% capacity retention after 1000 cycles [75,76].

In another study, L.-H. Hu et al. [76] found that carbon-coated LFPO doped with electrochemically exfoliated graphene has a specific capacity of 208 $mAh·g^{-1}$, above the theoretical limit of 170 $mAh·g^{-1}$ for conventional LFPO. The conductive graphene sheets increased electron mobility while decreasing capacity loss during cycling, demonstrating the potential for increased capacity retention and efficiency [76].

To balance the mechanical and electrochemical stability of both components, the combination of these two materials—Si/G anodes and $LiFePO_4$ cathodes—must be carefully tuned. Despite these challenges, integration is a topic of ongoing research in the field of advanced LIBs since it provides better energy densities by leveraging the superior electrochemical properties of LFPO and Si's high theoretical capacity.

## 4. ELECTROLYTE SOLUTIONS FOR SILICONE/GRAPHENE ANODES

The electrolyte plays a similar role in ion transport and interphase formation regardless of the Si-based electrode material. Selecting the appropriate electrolyte is essential because Si/G materials undergo substantial volume expansion and have a high reactivity with conventional electrolytes, which can cause degradation. The most promising electrolyte choices for improving Si/G anode performance will be covered in this section.

Ionic liquid electrolytes, especially those based on pyrrolidinium, have benefits including remarkable thermal stability and non-flammability that improve performance and safety at high temperatures. Under harsh operating circumstances, these electrolytes help to improve cycling stability by promoting the development of a stable SEI on Si/G anodes. When combined with fluoroethylene carbonate (FEC), lithium bis(fluorosulfonyl)imide (LiFSI) salts show better SEI formation properties and thermal stability than conventional $LiPF_6$ electrolytes. LiFSI exhibits reduced reactivity with the Si/G anode surface, which reduces electrolyte breakdown and improves battery performance even further [77].

Gel polymer electrolytes (GPEs), which frequently include FEC and vinylene carbonate (VC), offer a compromise between the stability of solid-state materials and the advantages of liquid electrolytes. GPEs can efficiently support Si/G anode growth while preserving ionic conductivity and flexibility, making them suitable for high-performance applications [77]. Moreover, hybrid electrolytes combine solid-state or gel components with conventional liquid electrolyte systems to provide a balance of stability and flexibility. These hybrid systems are a viable choice for cutting-edge battery technologies that use Si/G anodes since they are made to reduce electrolyte degradation, increase SEI stability, and increase overall safety [77].

Furthermore, the SEI on the Si/G surface is stabilized in large part by fluorinated electrolytes, especially those that use lithium hexafluorophosphate ($LiPF_6$) in combination with additives like FEC. FEC reduces irreversible capacity loss by forming a stable and flexible SEI that can handle the significant volume fluctuations associated with silicon during lithiation and delithiation cycles. The stability of the SEI is further increased when combined with VC, which improves cycling performance and extended battery life [77].

The main problem is that these solvents are chemically unstable during charge-discharge cycles, which can cause an uneven SEI to form on the anode surface. The anode materials' lifespan and efficiency are frequently shortened as a result of this instability. Furthermore, the mechanical load on the SEI layer is increased by the volumetric expansion of silicon during the lithiation and delithiation processes, leading to fissures and additional deterioration. Although FEC, VC and propylene carbonate (PC) are added to improve the stability of the SEI, the ongoing development and reformation of the SEI layer may reduce their efficacy [78].

Additionally, maintaining the chemical and mechanical stability of these solvents as well as enhancing the scalability of production processes are essential to the commercial feasibility of Si/G anodes. To address these problems and improve the overall performance and longevity of Si/G anodes, methods such sophisticated material production, exact control of solvent mixes, and creative electrode design are being investigated [78].

To create binary or ternary electrolytes and thoroughly examine their electrochemical performance in $LiNi_{0.5}Co_{0.2}Mn_{0.3}O_2$/Si-graphite full-cells, E. Zhao et al. [79] used FEC as their primary solvent. Consequently, the cells with FEC-based electrolytes exhibit good rate capacity retention under high current (up to 5 C) at room temperature and better specific capacities at 55 °C for the 200 cycles galvanostatic cycle test. Particularly noteworthy are the full-cells' low-temperature capabilities; of the investigated samples, the FEC/dimethyl carbonate (DMC) (5:5) electrolyte exhibits an exceptional capacity of up to 92.3 $mAh \cdot g^{-1}$ at 40 °C. Such FEC-based electrolytes would have enormous promise for Si/C anodes [79].

For freestanding Si-carbon nanotubes (CNTs) composite paper anodes for LIBs, researchers in Ref. [80] compared an electrolyte with FEC as the additive (10 wt.%) with another electrolyte type ethylene carbonate (EC) that used FEC as the co-solvent (50 wt.%). 1 M $LiPF_6$ in EC:DEC:FEC at a weight ratio of 45:45:10, 1 M $LiPF_6$ in EC:FEC at a weight ratio of 1:1, and 1 M $LiPF_6$ in DEC:FEC at a weight ratio of 1:1 are the particular electrolyte compositions that were examined. The designations for these three electrolytes are FEC 10%, EC-FEC, and DEC-FEC, in that order. In comparison to cells using EC-DEC-FEC (45:45:10 w/w/w) and EC-FEC (1:1 w/w), the capacity retention of the cell employing diethyl carbonate (DEC)-FEC (1:1 w/w) is enhanced by 88% and 60%, respectively, after 500 cycles [80]. The production of more polyolefins, which inhibit Li ion movement, is probably the cause of the poorer cell performance associated with the electrolytes containing EC [80].

Combining the polymer of GPE with inorganic materials in the form of transition metal oxide NPs allowed to improve the performance as well as the ionic conductivity. The metal oxide surface can act as an additional coordination center for $Li^+$ ions, which contributes to better cation transport. Specific ionic conductivity of the GPE containing 0.1 wt.% CuO NPs was 5.85 mS/cm, that is a high value comparable to the specific ionic conductivity of liquid organic electrolytes [81].

## 5. CONCLUSION

In this review, we investigated the potential of Si/G composite anodes for LIBs, focusing on their benefits, limitations, and recent improvements. Silicon anodes have outstanding theoretical capacity, but they confront substantial obstacles like as volume expansion during cycling, which reduces stability. Graphene anodes, on the other hand, have tremendous electrical conductivity and mechanical flexibility but lack the capacity needed for high-energy applications. Si/G composites, which combine the complimentary characteristics of silicon and graphene, offer a possible solution to these restrictions, providing increased capacity retention, structural stability, and rate performance.

Additionally, we looked at how important electrolytes are to maintaining compatibility with high-performance anodes. In particular, it has been determined that the electrolyte containing $LiPF_6$ in EC, DEC, and FEC is a good option for improving cycling stability and reducing adverse reactions. This arrangement shows promise for long-lasting and high-capacity LIBs that are appropriate for contemporary energy storage applications when combined with a $LiFePO_4$ cathode.

Si/G composites have a lot of potential, but more work is required to maximize their synthesis, scalability, and integration with cutting-edge cathodes and electrolytes. To solve outstanding issues and hasten the integration of Si/G-based LIBs in next-generation energy storage systems, more research and development in this area are essential.

## ACKNOWLEDGEMENTS

The study was supported by the RF Ministry of Science and Higher Education (project 075-15-2021-1349).

## REFERENCES

[1] J. Reslan, M. Saadaoui, T. Djenizian, Synthesis and Structural Design of Graphene, Silicon and Silicon-Based Materials Including Incorporation of Graphene as Anode to Improve Electrochemical Performance in Lithium-Ion Batteries, *Adv. Mater. Interfaces*, 2024, vol. 11, no. 19, pp. 1–25.

[2] H. Chang, Y.-R. Wu, X. Han, T.-F. Yi, Recent developments in advanced anode materials for lithium-ion batteries, *Energy Mater.*, 2022 ,vol. 1, no. 1, art. no. 100003.

[3] M.H. Hossain, M.A. Chowdhury, N. Hossain, M.A. Islam, M.H. Mobarak, Advances of lithium-ion batteries anode materials – A review, *Chem. Eng. J. Adv.*, 2023, vol. 16, art. no. 100569.

[4] S.K. Sharma, G. Sharma, A. Gaur, A. Arya, F.S. Mirsafi, R. Abolhassani, H.-G.Rubahn, J.-S.Yu,Y.K. Mishra, Progress in electrode and electrolyte materials: path to all-solid-state Li-ion batteries, *Energy Adv.*, 2022, vol. 1, no. 8, pp. 457–510.

[5] E. Podlesnov, M.G. Nigamatdianov, M.V. Dorogov, Review of Materials for Electrodes and Electrolytes of Lithium Batteries, *Rev. Adv. Mater. Technol.*, 2022, vol. 4, no. 4, pp. 39–61.

[6] A. Eftekhari, Low voltage anode materials for lithium-ion batteries, *Energy Storage Mater.*, 2017, vol. 7, pp. 157–180.

[7] P.U. Nzereogu, A.D. Omah, F.I. Ezema, E.I. Iwuoha, A.C. Nwanya, Anode materials for lithium-ion batteries: A review, *Appl. Surf. Sci. Adv.*, 2022, vol. 9, art. no. 100233.

[8] L. Ji, Z. Lin, M. Alcoutlabi, X. Zhang, Recent developments in nanostructured anode materials for rechargeable lithium-ion batteries, *Energy Environ. Sci.*, 2011, vol. 4, no. 8, pp. 2682–2689.

[9] J.K. Lee, C. Oh, N. Kim, J.Y. Hwang, Y.K. Sun, Rational design of silicon-based composites for high-energy storage devices, *J. Mater. Chem. A*, 2016, vol. 4, no. 15, pp. 5366–5384.

[10] H.J. Kim, T. Krishna, K. Zeb, V.Rajangam, C.V.V.M. Gopi, S. Sambasivam, K.V.G. Raghavendra, I.M. Obaidat, A comprehensive review of li-ion battery materials and their recycling techniques, *Electronics*, 2020, vol. 9, no. 7., art. no. 1161.

[11] A.R. Kamali, D.J. Fray, Tin-based materials as advanced anode materials for lithium ion batteries: A review, *Rev. Adv. Mater. Sci.*, 2011, vol. 27, no. 1, pp. 14–24.

[12] G.F.I. Toki, M.K. Hossain, W.U. Rehman, R.Z.A. Manj, L. Wang, J. Yang, Recent progress and challenges in silicon-based anode materials for lithium-ion batteries, *Ind. Chem. Mater.*, 2024, vol. 2, no. 2, pp. 226–269.

[13] *Si/C Composites for Battery Materials*, Electronic resource, URL: https://www.acsmaterial.com/blog-detail/sic-composites-for-battery-materials.html (accessed: 03.12.2024).

[14] A. Ulvestad, J.P. Mæhlen, M. Kirkengen, Silicon nitride as anode material for Li-ion batteries: Understanding the SiNx conversion reaction, *J. Power Sources*, 2018, vol. 399, no. 2027, pp. 414–421.

[15] M. Nie, D.P. Abraham, Y. Chen, A. Bose, B.L. Lucht, Silicon solid electrolyte interphase (SEI) of lithium ion battery characterized by microscopy and spectroscopy, *J. Phys. Chem. C*, 2013, vol. 117, no. 26, pp. 13403–13412.

[16] E. Feyzi, A. Kumar M R, X. Li, S. Deng, J. Nanda, K. Zaghib, A comprehensive review of silicon anodes for high-energy lithium-ion batteries: Challenges, latest developments, and perspectives, *Next Energy*, 2024, vol. 5, art. no. 100176.

[17] T.Vorauer, J.Schöggl, S.G. Sanadhya, M. Poluektov, W.D. Widanage, L. Figiel, S. Schädler, B. Tordoff, B. Fuchsbichler, S. Koller, R. Brunner, Impact of solid-electrolyte interphase reformation on capacity loss in silicon-based lithium-ion batteries, *Commun. Mater.*, 2023, vol. 4, no. 1, art. no. 44.

[18] X. Zhang, J. Weng, C. Ye, M. Liu, C. Wang, S. Wu, Q. Tong, M. Zhu, F. Gao, Strategies for Controlling or Releasing the Influence Due to the Volume Expansion of Silicon inside Si−C Composite Anode for High-Performance Lithium-Ion Batteries, *Materials*, 2022, vol. 15, no. 12, art. no. 4264.

[19] C. Zhang, F. Wang, J. Han, S. Bai, J. Tan, J. Liu, F. Li, Challenges and Recent Progress on Silicon-Based Anode Materials for Next-Generation Lithium-Ion Batteries, *Small Struct.*, 2021, vol. 2, no. 6, art. no. 2100009.

[20] F. De Santiago, J.E. González, A. Miranda, A. Trejo, F. Salazar, L.A. Pérez, M. Cruz-Irisson, Lithiation effects on the structural and electronic properties of Si nanowires as a potential anode material, *Energy Storage Mater.*, 2019, vol. 20, pp. 438–445.

[21] C. Yang, K.S.R. Chandran, A critical review of silicon nanowire electrodes and their energy storage capacities in Li-ion cells, *RSC Adv.*, 2023, vol. 13, no. 6, pp. 3947–3957.

[22] X. Li, M. Wu, T. Feng, Z. Xu, J. Qin, C. Chen, C. Tu, D. Wang, Graphene enhanced silicon/carbon composite as anode for high performance lithium-ion batteries, *RSC Adv.*, 2017, vol. 7, no. 76, pp. 48286–48293.

[23] B.A. Nuhu, O. Bamisile, H. Adun, U.O. Abu, D. Cai, Effects of transition metals for silicon-based lithium-ion battery anodes: A comparative study in electrochemical applications, *J. Alloys Compd.*, 2023, vol. 933, art. no. 167737.

[24] P. Hu, M. Dorogov, Y. Xin, K.E. Aifantis, Transforming Single-Crystal CuO/$Cu_2O$ Nanorods into Nano-Polycrystalline Cu/$Cu_2O$ through Lithiation, *ChemElectroChem*, 2019, vol. 6, no. 12, pp. 3139–3144.

[25] W. Wang, M.K. Datta, P.N. Kumta, Silicon-based composite anodes for Li-ion rechargeable batteries, *J. Mater. Chem.*, 2007, vol. 17, no. 30, pp. 3229–3237.

[26] M. Nigamatdianov, N. Chirkunova, M. Dorogov, Belt-like $SnO_2$ structures for lithium batteries, *AIP Conf. Proc.*, 2022, vol. 2533, no. 1, art. no. 020010.

[27] T. Insinna, E. N. Bassey, K. Märker, A. Collauto, A.L. Barra, C.P. Grey, Graphite Anodes for Li-Ion Batteries: An Electron Paramagnetic Resonance Investigation, *Chem. Mater.*, 2023, vol. 35, no. 14, pp. 5497–5511.

[28] *Silicon/Carbon (Si/C) Composite Anode Materials*, Electronic resource, URL: https://www.novarials.com/products/silicon-carbon-composite-anode-materials/ (accessed: 03.12.2024)

[29] Z. Chen, I. Belharouak, Y.K. Sun, K. Amine, Titanium-based anode materials for safe lithium-ion batteries, *Adv. Funct. Mater.*, 2013, vol. 23, no. 8, pp. 959–969.

[30] L. Zhong, C. Beaudette, J. Guo, K. Bozhilov, L. Mangolini, Tin nanoparticles as an effective conductive additive in silicon anodes, *Sci. Rep.*, 2016, vol. 6, art. no. 30952.

[31] A.G. Hailu, A. Ramar, F.-M. Wang, N.-H. Yeh, P.-W. Tiong, C.-C. Hsu, Y.-J. Chang, M.-M. Chen, T.-W. Chen, C.-C. Wang, B.A. Kahsay, L. Merinda, The development of super electrically conductive Si material with polymer brush acid and emeraldine base and its auto-switch design for high-safety and high-performance lithium-ion battery, *Electrochim. Acta*, 2022, vol. 429, art. no. 140829.

[32] Y. Javadzadeh, S. Hamedeyaz, Floating Drug Delivery Systems for Eradication of Helicobacter pylori in Treatment of Peptic Ulcer Disease, in: B. Roesler (Eds.), *Trends in Helicobacter pylori Infection*, InTech, 2014, pp. 303–319.

[33] D. Lou, S. Chen, S. Langrud, A.A. Razzaq, M. Mao, H. Younes, W. Xing, T. Lin, H. Hong, Scalable Fabrication of Si-Graphene Composite as Anode for Li-ion Batteries, *Appl. Sci.*, 2022, vol. 12, no. 21, art. no. 10926.

[34] J.C. Hestenes, J.T. Sadowski, R. May, L.E. Marbella, Transition Metal Dissolution Mechanisms and Impacts on Electronic Conductivity in Composite $LiNi_{0.5}Mn_{1.5}O_4$ Cathode Films, *ACS Mater. Au*, 2023, vol. 3, no. 2, pp. 88–101.

[35] H. Huo, M. Jiang, Y. Bai, S. Ahmed, K. Volz, H. Hartmann, A. Henss, C.V. Singh, D. Raabe, J. Janek, Chemo-mechanical failure mechanisms of the silicon anode in solid-state batteries, *Nat. Mater.*, 2024, vol. 23, no. 4, pp. 543–551.

[36] S.K. Kim, H. Kim, H. Chang, B.-G. Cho, J. Huang, H. Yoo, H. Kim, H.D. Jang, One-Step Formation of Silicon-Graphene Composites from Silicon Sludge Waste and Graphene Oxide via Aerosol Process for Lithium Ion Batteries, *Sci. Rep.*, 2016, vol. 6, art. no. 33688.

[37] G.G. Eshetu, H. Zhang, X. Judez, H. Adenusi, M. Armand, S. Passerini, E. Figgemeier, Production of high-energy Li-ion batteries comprising silicon-containing anodes and insertion-type cathodes, *Nat. Commun.*, 2021, vol. 12, art. no. 5459.

[38] J. Saddique, M. Wu, W. Ali, X. Xu, Z.-G. Jiang, L. Tong, H. Zheng, W. Hu, Opportunities and challenges of nano Si/C composites in lithium ion battery: A mini review, *J. Alloys Compd.*, 2024, vol. 978, art. no. 173507.

[39] M. Khan, S. Yan, M. Ali, F. Mahmood, Y. Zheng, G. Li, J. Liu, X. Song, Y. Wang, Innovative Solutions for High-Performance Silicon Anodes in Lithium-Ion Batteries: Overcoming Challenges and Real-World Applications, *Nano-Micro Lett.*, 2024. vol. 16, art. no. 179.

[40] J. Liang, Y. Xu, H. Sun, X. Xu, T. Liu, H. Liu, H. Wang, Vacuum-Dried 3D Holey Graphene Frameworks Enabling High Mass Loading and Fast Charge Transfer for Advanced Batteries, *Energy Technol.*, 2020, vol. 8, no. 3, art. no. 1901002.

[41] Y. Cen, R. Sisson, Q. Qin, J. Liang, Current Progress of Si/Graphene Nanocomposites for Lithium-Ion Batteries, *C*, 2018, vol. 4, no. 1, art. no. 18.

[42] M. Jiao, Y. Wang, C. Ye, C. Wang, W. Zhang, C. Liang, High-capacity $SiO_x$ ($0 \leq x \leq 2$) as promising anode materials for next-generation lithium-ion batteries, *J. Alloys Compd.*, 2020, vol. 842, art. no. 155774.

[43] Q. Zhang, N.-J. Song, C.-L. Ma, Y. Zhao, Y. Li, J. Li, X.-M. Li, Q.-Q. Kong, C.-M. Chen, Constructing a Low-Cost Si–NSs@C/NG Composite by a Ball Milling-Catalytic Pyrolysis Method for Lithium Storage, *Molecules*, 2023, vol. 28, no. 8, art. no. 3458.

[44] M. Gauthier, D. Mazouzi, D. Reyter, B. Lestriez, P. Moreau, D. Guyomard, L. Roué, A low-cost and high performance ball-milled Si-based negative electrode for high-energy Li-ion batteries, *Energy Environ. Sci.*, 2013, vol. 6, no. 7, pp. 2145–2155.

[45] Q. Shi, J. Zhou, S. Ullah, X. Yang, K. Tokarska, B. Trzebicka, H.Q. Ta, M.H. Rümmeli, A review of recent developments in Si/C composite materials for Li-ion batteries, *Energy Storage Mater.*, 2021, vol. 34, pp. 735–754.

[46] Y. Cui, X. Duan, J. Hu, C.M. Lieber, Doping and Electrical Transport in Silicon Nanowires, *J. Phys. Chem. B*, 2000, vol. 104, no. 22, pp. 5213–5216.

[47] W. Ren, Y. Wang, Z. Zhang, Q. Tan, Z. Zhong, F. Su, Carbon-coated porous silicon composites as high performance Li-ion battery anode materials: Can the production process be cheaper and greener?, *J. Mater. Chem. A*, 2015, vol. 4, no. 2, pp. 552–560.

[48] A. Magasinski, P. Dixon, B. Hertzberg, A. Kvit, J. Ayala, G. Yushin, High-performance lithium-ion anodes using a hierarchical bottom-up approach, *Nat. Mater.*, 2010, vol. 9, no. 4, pp. 353–358.

[49] L.M. Dorogin, M.V. Dorogov, S. Vlassov, A.A. Vikarchuk, A.E. Romanov, Whisker Growth and Cavity Formation at the Microscale, *Rev. Adv. Mater. Technol.*, 2020, vol. 2, no. 1, pp. 1–31.

[50] M. Dorogov, A. Kalmykov, L. Sorokin, A. Kozlov, A. Myasoedov, D. Kirilenko, N. Chirkunova, A. Priezzheva, A. Romanov, E.C. Aifantis, CuO nanowhiskers: preparation, structure features, properties, and applications, *Mater. Sci. Technol.*, 2018, vol. 34, no. 17, pp. 2126–2135.

[51] E. Podlesnov, M.V. Dorogov, Nanowhiskers for lithium battery anode, *IOP Conf. Ser.: Mater. Sci. Eng.*, 2020, vol. 1008, art. no. 012043.

[52] A.R. Urade, I. Lahiri, K.S. Suresh, Graphene Properties, Synthesis and Applications: A Review, *JOM*, 2023, vol. 75, no. 3, pp. 614–630.

[53] Z. Liu, Y. Tian, P. Wang, G. Zhang, Applications of graphene-based composites in the anode of lithium-ion batteries, *Front. Nanotechnol.*, 2022, vol. 4, art. no. 952200.

[54] A. Islam, B. Mukherjee, K.K. Pandey, A.K. Keshri, Ultra-Fast, Chemical-Free, Mass Production of High Quality Exfoliated Graphene, *ACS Nano*, 2021, vol. 15, no. 1, pp. 1775–1784.

[55] A.R.R. Hernández, A.G. Cruz, J. Campos-Delgado, Chemical Vapor Deposition Synthesis of Graphene on Copper Foils, in: M. Ikram, A. Maqsood, A. Bashir (Eds.), *Graphene - A Wonder Material for Scientists and Engineers*, IntechOpen, 2023, pp. 1–16.

[56] *CVD Graphene | Technology | Chemical Vapor Deposition Graphene*, URL: https://generalgraphenecorp.com/technology/ (accessed: 03.12.2024).

[57] K. Rana, S.D. Kim, J.-H. Ahn, Additive-free thick graphene film as an anode material for flexible lithium-ion batteries, *Nanoscale*, 2015, vol. 7, no. 16, pp. 7065–7071.

[58] I. Imae, K. Yukinaga, K. Imato, Y. Ooyama, Y. Kimura, Facile silicon / graphene composite synthesis method for application in lithium-ion batteries, *Ceram. Int.*, 2022, vol. 48, no. 17, pp. 25439–25444.

[59] P.B. Zhang, Y. You, C. Wang, X.H. Fang, W. Ren, L.Y. Yang, X.Y. Chen, A novel anode material for lithium-ion batteries: silicon nanoparticles and graphene composite films, *IOP Conf. Ser.: Earth Environ. Sci.*, 2019, vol. 354, art. no. 12079.

[60] J.K. Lee, K.B. Smith, C.M. Hayner, H.H. Kung, Silicon nanoparticles–graphene paper composites for Li ion battery anodes, *Chem. Commun.*, 2010, vol. 46, no. 12, pp. 2025–2027.

[61] Y. Ye, X. Xie, J. Rick, F. Chang, B. Hwang, Improved anode materials for lithium-ion batteries comprise non-covalently bonded graphene and silicon nanoparticles, *J. Power Sources*, 2014, vol. 247, pp. 991–998.

[62] D.C. Marcano, D.V. Kosynkin, J.M. Berlin, A. Sinitskii, Z. Sun, A. Slesarev, L.B. Alemany, W. Lu, J.M. Tour, Improved synthesis of graphene oxide, *ACS Nano*, 2010, vol. 4, no. 8, pp. 4806–4814.

[63] L. Niu, Q. Zhang, R. Zhang, D. Wang, G. Wen, L. Qin, Modulating functional groups of GO to improve the electrochemical performance of Si/rGO anode, *Colloids Surf. A Physicochem. Eng. Asp.*, 2024, vol. 691, art. no. 133877.

[64] W.S. Hummers Jr., R.E. Offeman, Preparation of graphitic oxide, *J. Am. Chem. Soc.*, 1958, vol. 80, no. 6, p. 1339.

[65] Y. Du, G. Zhu, K. Wang, Y. Wang, C. Wang, Y. Xia, Si/graphene composite prepared by magnesium thermal reduction of $SiO_2$ as anode material for lithium-ion batteries, *Electrochem. Commun.*, 2013, vol. 36, pp. 107–110.

[66] M.-S. Wang, Z.-Q. Wang, R. Jia, Y. Yang, F.-Y. Zhu, Z.-L. Yang, Y. Huang, X. Li, W. Xu, Facile electrostatic self-assembly of silicon/reduced graphene oxide porous composite by silica assist as high performance anode for Li-ion battery, *Appl. Surf. Sci.*, 2018, vol. 456, pp. 379–389.

[67] X. Zhang, D. Wang, X. Qiu, Y. Ma, D. Kong, K. Müllen, X. Li, L. Zhi, Stable high-capacity and high-rate silicon-based lithium battery anodes upon two-dimensional covalent encapsulation, *Nat. Commun.*, 2020, vol. 11, art. no. 3826.

[68] W. Zhang, S. Gui, W. Li, S. Tu, G. Li, Y. Zhang, Y. Sun, J. Xie, H. Zhou, H. Yang, Functionally gradient silicon/graphite composite electrodes enabling stable cycling and high capacity for lithium-ion batteries, *ACS Appl. Mater. Interfaces*, 2022, vol. 14, no. 46, pp. 51954–51964.

[69] S. Kaushik, T. Mehta, P. Chand, S. Sharma, G. Kumar, Recent advancements in cathode materials for high-performance Li-ion batteries: Progress and prospects, *J. Energy Storage*, 2024, vol. 97, part A, art. no. 112818.

[70] *What Are Battery Anode and Cathode Materials? – Aqua-Metals*, Electronic resource, URL: https://aquametals.com/recyclopedia/lithium-ion-anode-and-cathode-materials/ (accessed: 03.12.2024).

[71] *Cost-effective, high-capacity, and cyclable lithium-ion battery cathodes*, Electronic resource, URL: https://www.sciencedaily.com/releases/2024/05/240502141245.htm (accessed: 03.12.2024).

[72] Y. Lu, H. Han, Z. Yang, Y. Ni, Z. Meng, Q. Zhang, H. Wu, W. Xie, Z. Yan, J. Chen, High-capacity dilithium hydroquinone cathode material for lithium-ion batteries, *National Science Review*, 2024, vol. 11, no. 6, art. no. nwae146.

[73] J. Li, X. Zhang, R. Peng, Y. Huang, L. Guo, Y. Qi, $LiMn_2O_4$/graphene composites as cathodes with enhanced electrochemical performance for lithium-ion capacitors, *RSC Adv.*, 2016, vol. 6, no. 60, pp. 54866–54873.

[74] R. Hu, W. Sun, Y. Chen, M. Zeng, M. Zhu, Silicon/graphene based nanocomposite anode: large-scale production and stable high capacity for lithium ion batteries, *J. Mater. Chem. A*, 2014, vol. 2, no. 24, pp. 9118–9125.

[75] M.J. Loveridge, M.J. Lain, I.D. Johnson, A. Roberts, S.D. Beattie, R. Dashwood, J.A. Darr, R. Bhagat, Towards high capacity Li-ion batteries based on silicon-graphene composite anodes and sub-micron V-doped $LiFePO_4$ cathodes, *Sci. Rep.*, 2016, vol. 6, no. 1, art. no. 37787.

[76] M. Je, D.-Y. Han, J. Ryu, S. Park, Constructing pure Si anodes for advanced lithium batteries, *Acc. Chem. Res.*, 2023, vol. 56, no. 16, pp. 2213–2224.

[77] M.S. Ahmed, M. Islam, B. Raut, S. Yun, H. Y. Kim, K.-W. Nam, A Comprehensive Review of Functional Gel Polymer Electrolytes and Applications in Lithium-Ion Battery, *Gels*, 2024, vol. 10, no. 9, art. no. 563.

[78] J. Asenbauer, T. Eisenmann, M. Kuenzel, A. Kazzazi, Z. Chen, D. Bresser, The success story of graphite as a lithium-ion anode material–fundamentals, remaining challenges, and recent developments including silicon (oxide) composites, *Sustain. Energy Fuels*, 2020, vol. 4, no. 11, pp. 5387–5416.

[79] E. Zhao, Y. Gu, S. Fang, L. Yang, S. Hirano, Systematic investigation of electrochemical performances for lithium-ion batteries with Si/Graphite anodes: effect of electrolytes based on fluoroethylene carbonate and linear carbonates, *ACS Appl. Energy Mater.*, 2021, vol. 4, no. 3, pp. 2419–2429.

[80] K. Yao, J. P. Zheng, R. Liang, Ethylene carbonate-free fluoroethylene carbonate-based electrolyte works better for freestanding Si-based composite paper anodes for Li-ion batteries, *J. Power Sources*, 2018, vol. 381, pp. 164–170.

[81] E. Podlesnov, M.G. Nigamatdianov, A.O. Safronova, M.V. Dorogov, Lithium Polymer Battery with PVDF-based Electrolyte Doped with Copper Oxide Nanoparticles: Manufacturing Technology and Properties, *Rev. Adv. Mater. Technol.*, 2021, vol. 3 no 3, pp. 27–31.

УДК 621.355

# Изготовление композитных анодов Si/G для литий-ионных аккумуляторов: обзор

**А. Азаизия, М.В. Дорогов**

Институт перспективных систем передачи данных, Университет ИТМО, Кронверкский пр., 49, лит. А, Санкт-Петербург, 197101, Россия

**Аннотация.** Последние разработки в области композитных анодов из кремния и графена имеют большие перспективы в литий-ионных аккумуляторах благодаря преодолению ограничений их производительности. Кремний обладает высокой теоретической емкостью, однако во время циклирования происходит значительное изменение его объема. Графен известен превосходными механическими свойствами и электропроводностью, но у него малый потенциал для высокоэнергетических применений, однако он улучшает качества кремния. Благодаря объединению этих материалов такие композиты показывают впечатляющие результаты по производительности, структурной стабильности и сохранению емкости, что открывает возможности для разработки технологий хранения энергии нового поколения. Создание высокопроизводительных композитов стало проще благодаря достижениям в масштабируемых процессах синтеза, таких как золь-гель синтез, химическое осаждение из паровой фазы, методы самосборки и метод Хаммера. В обзоре рассмотрены последние разработки и нерешенные вопросы в литий-ионных аккумуляторах с акцентом на перспективные аноды на основе кремния, углеродные композиты и методы получения и исследования кремниевых анодов. Эти вопросы имеют решающее значение для удовлетворения потребностей современных устройств с высокой емкостью и ускорения внедрения композитов в системы хранения энергии нового поколения.

*Ключевые слова:* литий-ионные аккумуляторы; аноды на основе кремния; системы высокой емкости для хранения энергии; стабильность циклирования